Capture and Direct Amplification of DNA on Chitosan Microparticles in a Single PCR-Optimal Solution
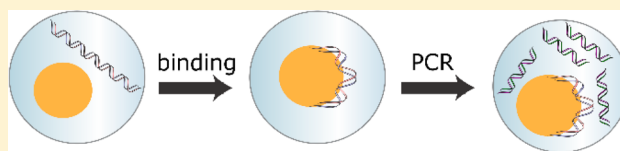
Kunal R. Pandit,[†,‡] Imaly A. Nanayakkara,[†,§] Weidong Cao,[∥] Srinivasa R. Raghavan,[‡,§] and Ian M. White*,[§]

[‡]Department of Chemical and Biomolecular Engineering and [§]Fischell Department of Bioengineering, University of Maryland, College Park, Maryland, United States

[∥]Canon U.S. Life Sciences, Inc., Rockville, Maryland, United States

Ⓢ Supporting Information

ABSTRACT: While nucleic acid amplification tests have great potential as tools for rapid diagnostics, complicated sample preparation requirements inhibit their use in near-patient diagnostics and low-resource-setting applications. Recent advancements in nucleic acid purification have leveraged pH-modulated charge switching polymers to reduce the number of steps required for sample preparation. The polycation chitosan (pK_a 6.4) has been used to efficiently purify DNA by binding nucleic acids in acidic buffers and then eluting them at a pH higher than 8.0. Though it is an improvement over conventional methods, this multistep procedure has not transformed the application of nucleic acid amplification assays. Here we describe a simpler approach using magnetic chitosan microparticles that interact with DNA in a manner that has not been reported before. The microparticles capture DNA at a pH optimal for PCR (8.5) just as efficiently as at low pH. Importantly, the captured DNA is still accessible by polymerase, enabling direct amplification from the microparticles. We demonstrate quantitative PCR from DNA captured on the microparticles, thus eliminating nearly all of the sample preparation steps. We anticipate that this new streamlined method for preparing DNA for amplification will greatly expand the diagnostic applications of nucleic acid amplification tests.

Nucleic acid amplification methods (e.g., the polymerase chain reaction or PCR) are powerful tools for biological research and disease diagnostics. While the amplification and quantification steps are mostly automated and straightforward, sample preparation can be complex, as DNA or RNA targets are normally diluted in a complex lysate or mixture from food, environmental, or clinical samples, suggesting the need for nucleic acid purification. Ultimately, it is the complexity of the sample preparation that prevents PCR-based techniques from being widely adopted away from the central laboratory.

Traditionally, nucleic acid purification is carried out using a solid phase extraction technique.[1−3] The most commonly used commercially available format is a spin column with a silica membrane designed for use with a centrifuge.[4] First, the tissue or cellular sample is lysed to release DNA with a chemical lysis buffer and agitation. Then, binding, washing, and elution solutions are driven through the column by centrifugal force in a series of steps. Nucleic acids in samples are denatured by chaotropic salts, such as guanidine hydrochloride, which cause adsorption to the silica. Alcohol is then used to wash away the salts and cellular debris, which would otherwise inhibit PCR. Purified nucleic acids are then eluted off of the silica in a moderate salt buffer and added to the amplification solution.

There are several inherent disadvantages to using silica membranes to purify nucleic acids. First, the numerous steps generally require hands-on processing, implying that PCR sample preparation for molecular diagnostics applications is limited to central laboratories; meanwhile, the automation of washes increases in complexity with the number of steps. In addition, the chaotropic agents and alcohols are inhibitory to amplification methods, making it a challenge to reduce the number of steps. Furthermore, commercial spin columns can process only relatively small samples, that is, on the order of 500 μL in volume. To capture dilute DNA or RNA from a rare target, the sample volume must be increased, leading to volumes that are impractical for spin columns.

Recently, the steps for solid phase extraction have been adapted for silica microparticles. The surface of the microparticles takes the place of the silica membrane; meanwhile, microparticles enable the elimination of one step from the process by lysing cells and capturing the released DNA under vortex in the presence of a high concentration of chaotropic salts. In addition, the use of magnetic microparticles may simplify the procedure.[5] Nonetheless, even with the elimination of a step, the method is still relatively complex and time-consuming and does not position PCR methods for use away from the central lab.

Another method that has been reported to reduce the number of sample preparation steps is charge switching. In this approach, nucleic acids are captured onto a pH-responsive

material in a moderately low pH (in which the material is cationic) and then released into a moderately high pH (compatible with PCR), which neutralizes the binding material.[6] Thus, in the charge switching methodology, inhibitory salt concentrations, chaotropic salts, and solvents are not necessary. Instead, buffers compatible with PCR are used for the release, which reduces steps and eliminates the use of inhibiting reagents.[7] Also, the charge switching format can be easily adapted to a particle geometry to process large volumes.[7−9]

Chitosan is a particularly useful polycation for charge-switching due to its abundance of amine groups that can be charge-modulated via pH. It is a derivative of chitin extracted from crustacean shells and thus is readily available, inexpensive, and biocompatible. The amine group on chitosan has a pK_a of about 6.4; hence, chitosan is cationic at pH below 6.4 and can readily bind the anionic DNA under these conditions. Chitosan also readily forms nanoparticle complexes with nucleic acids which can be used as gene and siRNA transfection vehicles.[10,11] Low molecular weight chitosan oligosaccharide functionalized silica particles have been shown to efficiently elute DNA at a moderately high pH (∼8.5) compatible with PCR. Additionally, chitosan-coated silica particles under aqueous conditions have been shown to extract RNA from cancer cells more efficiently than bare silica particles.[8] Chitosan-coated silica particles have also been used to purify genomic DNA from blood[7] and soybeans[12] for PCR analysis. However, while the use of charge switching implies a reduction in steps (lyse, bind, elute) as compared to silica membranes, the number of steps continues to imply complexity in attempts for automation and, as a result, has not led to near-patient PCR-based diagnostics.

Further simplification can be achieved by eliminating the elution step altogether. In this paradigm, the surface would bind DNA and retain DNA during any washes, such that the binding material could be directly transferred to a PCR reaction with the nucleic acids still bound to the solid phase. For example, aluminum oxide membranes have been shown to bind nucleic acids at high salt concentrations similarly to solid silica supports. Although it is difficult to elute the nucleic acid off, bound DNA can be amplified with the membrane in the reaction solution.[13,14] However, it was also shown in that same work that alumina inhibits PCR, and thus the exposed surface area must be minimized. This limits its potential for practical implementation.

More recently, commercially available magnetic particles have been demonstrated to capture nucleic acids at high pH (with NaOH added) and to retain the nucleic acids in a wash with pH-compatible buffer.[15] The microparticles can be added directly to a PCR reaction without significant inhibition. Thus, the lyse/adsorb steps can be combined, while the elution step can be eliminated. While this approach is significantly simpler than conventional solid phase extraction, elimination of the requirement for a high-pH NaOH binding solution would lead to a protocol that can be completely automated and utilized away from the central laboratory.

Here we report a new approach that allows DNA capture and subsequent amplification to be performed in a single solution that is optimal for PCR. As described above, chitosan has a pK_a of 6.4, and thus, chitosan-treated surfaces release nucleic acids in PCR-compatible solutions. However, it has been shown that, in a dense chitosan microenvironment, the pK_a can be shifted in the presence of anionic molecules, including nucleic acids.[16,17] We leverage this phenomenon to perform (i) adsorption of

DNA in a solution that is optimized for PCR and (ii) subsequent amplification of the captured DNA directly from the chitosan. To accomplish this, we utilized magnetic microparticles fabricated from chitosan. The interior of the microparticles was shown to maintain a positive charge at PCR-compatible pH, thus retaining genomic DNA captured just below the surface under vortex conditions, while the outer surface was shown to exhibit the characteristic charge switching properties of chitosan, thereby not inhibiting the PCR reaction. We demonstrated that plasmid DNA is captured at pH 8.5 and is efficiently amplified directly from the microparticle substrate with PCR. This new methodology for sample preparation has the potential to lead to a simple and automated technique for PCR sample preparation, which may have significant impact on near-patient molecular diagnostics.

■ EXPERIMENTAL SECTION

Microparticle Fabrication. Chitosan microparticles were fabricated by creating aqueous chitosan droplets in oil and then cross-linking the droplets into microparticles. Stock solutions of 2% (w/w) low molecular weight chitosan (Sigma) in 2% (v/v) acetic acid (Fisher) and an oil solution of 2% (w/w) Span 80 (Fluka) in hexadecane (Sigma) were prepared and stored at room temperature. Prior to microparticle fabrication, an aqueous solution of 1% (w/w) low molecular weight chitosan and 0.5% (w/w) magnetic iron(III) oxide nanoparticles, 20−40 nm in diameter (Alfa Aesar) in 1% (v/v) acetic acid, was prepared. A cross-linking solution of 0.44 g glutaraldehyde (grade 1, 70% in H_2O, Sigma) in 1 mL of oil solution was also prepared. Chitosan was emulsified in a 100 mL beaker by dripping 1 mL of the aqueous solution into 19 mL of the oil solution under constant mixing with an IKA T25 digital ULTRA-TURRAX homogenizer set at 1600 rpm. After emulsifying for 3 min, the cross-linking mixture was added dropwise and then further mixed with the homogenizer for an additional 5 min. Microparticles were cross-linked by glutaraldehyde, which reacts with chitosan amine groups to form Schiff bases.[18] Next, the microparticles were transferred to a 50 mL tube and cross-linked for the desired amount of time on a nutating rocker. The cross-linking reaction was stopped by removing the glutaraldehyde-laden hexadecane after the microparticles were centrifuged at 1000 rpm for 2 min.

To prepare the microparticles for DNA adsorption assays they were first washed twice with oil solution. Then the microparticles were resuspended in oil solution and dried with an air stream bubbling through the solution overnight. The oil solution was removed by washing the beads twice, first in decanol (Alfa Aesar), then ethanol (Pharmco-AAPER), and finally 10 mM Tris (Sigma). Schiff bases, which cross-linked the microparticles, were then reduced to secondary amines in 1% (w/w) $NaBH_4$ (Sigma) in 10 mM Tris overnight.[18] After reduction, the microparticles were washed twice in 10 mM Tris. Finally, they were dried overnight at room temperature under vacuum. Chitosan microparticles were stored in 10 mM Tris (pH 8.5) at a concentration of 40 mg/mL at 4 °C.

DNA Capture below pK_a. Quantitative DNA capture assays at pH 5 were performed by a series of buffer changes in 600 μL microtubes with qPCR quantification of DNA in each supernatant. First, 40 μg of chitosan microparticles (cross-linked for 30 min) were washed twice with loading buffer (pH 5, 10 mM MES, 0.1% (w/w) Triton X-100). Next, 1 μL of pUC19 plasmid DNA (Sigma) or *E. coli* genomic DNA (Sigma) diluted in deionized (DI) H_2O was added to 99 μL of

loading buffer containing the chitosan microparticles. Then the microparticles were washed in 100 μL of load buffer. Lastly, the beads were vortexed in 100 μL elution buffer (pH 9, 10 mM Tris, 0.1% (w/w) Triton X-100 (Sigma) and 50 mM KCl) on the highest speed for 3 min. All buffer changes were facilitated by a magnetic tube stand that pulled and held the magnetic chitosan microparticles to one side of the tube. Supernatants from each step were preserved for qPCR analysis.

PCR-Compatible-pH Capture. DNA adsorption assays at PCR-compatible pH (8.5) were similar to the assay at lower pH. First, 40 μg of chitosan microparticles cross-linked for 30 min were prewashed twice in pH 8.5 loading buffer (10 mM Tris, 0.1% (w/w) Triton X-100). To wash the microparticles, the tube was held on a magnetic stand, which pulled the microparticles to the side of the tube, enabling the supernatant to be aspirated; no centrifugation was used. DNA was loaded onto the microparticles by adding 1 μL of pUC19 plasmid DNA or *E. coli* genomic DNA diluted in DI H$_2$O to 99 μL of load buffer (pH 8.5). Lastly, the beads were washed in 100 μL of load buffer (pH 8.5). The amount of DNA in the supernatants at each step was quantified with qPCR.

qPCR. To quantify the amount of DNA captured or released in each step, the respective supernatants were analyzed with qPCR using an MJ MiniOpticon thermal cycler (BioRad). Reactions consisted of 10 μL of iQ SYBR Green Supermix (BioRad), 2 μL of 2.5 μM forward primer (GTC TCA TGA GCG GAT ACA A), 2 μL of 2.5 μM reverse primer (CTC GTG ATA CGC CTA TTT TT, primers purchased from IDT), and 6 μL of samples. PCR reactions utilized a hot-start at 95 °C for 3 min followed by 30 thermal cycles. Each cycle included a melt step at 95 °C for 3 s and an anneal step at 56 °C for 30 s. Serial dilutions of pUC19 plasmid DNA in load and elution buffers were used to generate a calibration curve to quantify the unknown samples. Reported cycle thresholds are the values provided by the PCR system.

Elution under Extreme Conditions. To investigate the binding strength of DNA to the chitosan microparticles, multiple elution steps, high ionic strength, high pH, and high temperature elution washes, were performed after microparticles (cross-linked for 30 min) were loaded with pUC19 plasmid DNA and washed. Additional washes with elution buffer were performed to increase the probability of eluting DNA. High ionic strength conditions were examined by vortexing beads in 100 μL of pH 8.5, 10 mM Tris, 0.1% (w/w) Triton X-100, and up to 500 mM KCl for 3 min. High pH conditions were examined by vortexing microparticles in Tris, bicarbonate, or sodium hydroxide buffers at a concentration of 10 mM and up to pH 12.5 for 3 min. High temperature elution was examined by suspending the beads in 100 μL of elution buffer and thermal cycling them according to the qPCR protocol with an additional 95 °C hold step at the end. The supernatant was removed during the hold step and released DNA was quantified with qPCR.

Adsorption Mechanism Assays. The adsorption of the anionic dye brilliant yellow (Sigma), BY, to chitosan particles at increasing pH was measured to investigate electrostatic interactions. Solutions of BY in 10 mM buffers and 0.1% (w/w) Triton X-100 from pH 5 to 12.5 served as standards and load samples. First, 40 μg of chitosan microparticles cross-linked for 30 min or 24 h were prewashed twice in buffer without BY. Then 100 μL of 50 μM BY was loaded onto the microparticles. After vortexing for 3 min, BY remaining in the supernatant was quantified by comparing the absorbance at 397

nm with an Evolution 60 spectrophotometer to standard solutions. Each recorded value represents an average of three trials. The adsorption of methylene blue (Sigma) to chitosan microparticles cross-linked for 30 min (absorbance measured at 670 nm) was also measured in the same manner as BY to serve as a control.

The adsorption of negatively charged gold nanoparticles to chitosan microparticles cross-linked for 30 min was measured to determine the charge exclusively at the surface of the microparticles. Gold nanoparticles were synthesized by boiling chloroauric acid with sodium citrate.[19] Just as with BY, gold nanoparticles remaining in the supernatant after vortexing with chitosan microparticles were quantified (absorbance measured at 530 nm). The buffer strength was reduced to 5 mM Tris when measuring gold nanoparticle adsorption. The adsorption at pH 6 and 8.5 were examined.

Direct PCR Amplification of Microparticle-Adsorbed DNA. To demonstrate that DNA can be amplified directly from the chitosan microparticles, chitosan microparticles (30 min cross-link time) were added to a PCR reaction immediately after DNA adsorption. The reaction mixture consisted of 1.4× iQ SYBR Green Supermix, 0.36 μM forward primer, and 0.36 μM reverse primer. Following DNA capture at pH 8.5, the microparticles were resuspended in 30 μL of pH 8.5 loading buffer and transferred to a PCR well. The loading buffer was replaced with 20 μL of reaction mixture and then aspirated via pipet. Bubbles in the wells were removed by centrifugation. A magnet was used to disperse particles throughout the well after centrifugation and to ensure they were not tightly packed at the bottom. Magnets were also placed inside the thermal cycler adjacent to wells during PCR, which held particles to one side of a well and allowed for real-time fluorescence measurements. The reactions were thermal cycled as described earlier for 35 cycles. Each data point on the calibration curve is an average of three trials (using three different load samples).

Primer Adsorption to Microparticles. Primer adsorption to chitosan microparticles was investigated by conducting PCR with a primer solution that had been mixed with chitosan microparticles. First, 40 μg of chitosan microparticles cross-linked for 30 min was prewashed twice in pH 8.5 loading buffer. Then 100 μL of 10 mM Tris, 2.5 μM forward primer, 2.5 μM reverse primer, and 0.1% (w/w) Triton X-100 at pH 8.5 was repeatedly aspirated with the microparticles via pipet to mix the solution. The supernatant containing primers that did not bind to the microparticles was removed and used for qPCR. Reaction mixtures consisted of 10 μL iQ SYBR Green Supermix, 2 μL of primer solution, 2 μL DI H$_2$O, and 6 μL of pUC19 standards.

PCR Product Identification. Thermal melt analysis and gel electrophoresis were utilized on the supernatants obtained following PCR reactions with chitosan microparticles to verify PCR products. The melt analysis was conducted immediately after PCR within the same thermal cycler. The temperature was increased from 65 to 95 °C every 5 s by 0.5 °C and the fluorescence was measured at each temperature step. Also, the supernatant from direct PCR was separated on a 1% (w/w) agarose (BioRad) and 1.6× SYBR Green I (Lonza) gel at 75 V for 1.5 h.

■ RESULTS AND DISCUSSION

Chitosan Microparticle Fabrication. Aldehydes readily react with amines to form labile Schiff bases. Thus, intermolecular and intramolecular bonds between chitosan

amine groups are formed when exposed to glutaraldehyde (Figure 1). These bonds are reduced to covalent bonds with a
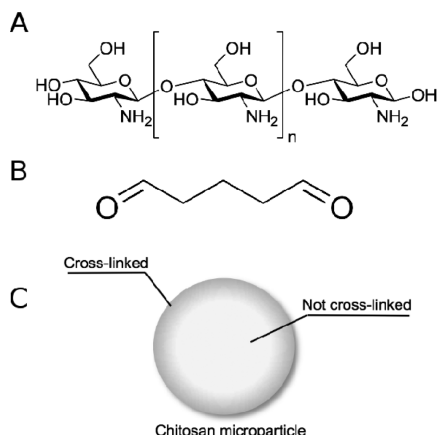

Figure 1. (A) Structure of chitosan. (B) Structure of glutaraldehyde. (C) Predicted structure of cross-linked microparticle, in which chitosan is cross-linked by glutaraldehyde from the outside in.

reducing agent such as NaBH$_4$. We utilized these reactions by immersing aqueous chitosan droplets in glutaraldehyde-laden oil. Thus, the droplets were cross-linked into particles, where the reaction began at the oil−water interface and continued toward the core of the particle over time (Figure 1).

Magnetic chitosan microparticles were fabricated using a facile emulsion cross-linking methodology. We observed the particles to be dispersed while cross-linking, washing, and drying in hexadecane. However, the particles aggregated into larger particles when washed with solvents other than hexadecane. Furthermore, large clusters of particles were formed after drying under vacuum, which were broken down by sonication. SEM images of the final freeze-dried chitosan particle product (Figure 2) showed individual microparticles clustered into larger particles. Individual particles were narrowly polydisperse and ranged in diameter from 0.5 to 8 μm. A large
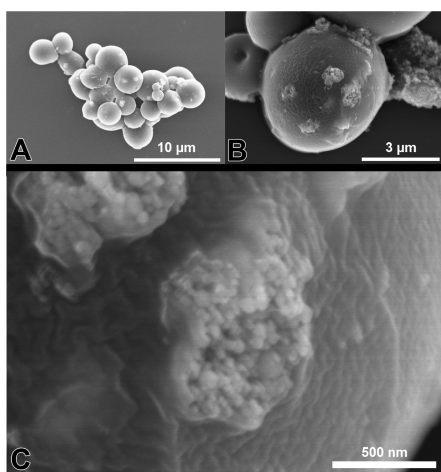

Figure 2. SEM images of whole chitosan particles cross-linked for 30 min. (A) Individual particles ranged in diameter from 0.5 to 8 μm. A majority of the particles were clustered into aggregates on the order of 10 μm. (B) A cluster of particles with iron(III) oxide nanoparticles, 20−40 nm in diameter, is visible. (C) Magnified view of iron(III) oxide nanoparticles embedded within the chitosan matrix of the particle.

majority of the particles were clustered into particles on the order of 10 μm, although single particles were not uncommon. Magnetic iron nanoparticles, 20−40 nm in diameter, were found embedded within individual microparticles (Figure 2C). The particles were very responsive to magnets in close proximity, which allowed for quick buffer changes. Also, the particles were opaque and rust colored from the magnetic nanoparticles and fluoresced under blue light.

DNA Adsorption onto Chitosan Microparticles. To assess the capture and release of DNA with the chitosan microparticles, the supernatant was subjected to qPCR after vortexing DNA with the microparticles and after washing (i.e., attempted elution). The results of each qPCR for various conditions are presented in Figure 3. Consistent with
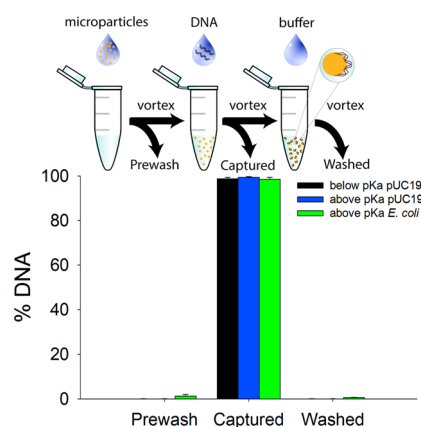

Figure 3. Permanent capture of DNA onto chitosan microparticles at pH below the pK_a (5.0) and above the pK_a (8.5). DNA was quantified by performing qPCR on the supernatant. The amount of captured DNA is determined by subtracting the quantified amount of DNA in the supernatant from the amount of loaded DNA.

previously published work on chitosan for DNA purification, our chitosan microparticles efficiently captured DNA from acidic buffers. However, in contrast to the chitosan-based charge-switching reports in which solid supports were functionalized with oligomeric chitosan,[7,20] DNA did not elute from the chitosan microparticles at a pH above the pK_a (e.g., 8.5). Further washing of the microparticles with elution buffer multiple times did not result in release of pUC19 into solution. Kendall et al., also reported that densely coated microporous chitosan monoliths exhibited poor pUC19 DNA elution at a pH in the range of 8.5.[21] We attempted to elute DNA off of the microparticles at more extreme elution conditions by (i) increasing the ionic strength, (ii) increasing the pH, and (iii) increasing the temperature by subjecting the beads to 30 PCR thermal cycles including a hot-start step. None of these enhanced elution conditions resulted in released DNA that could be measured via qPCR. This indicated that extreme elution conditions did not diminish the interactions between the chitosan microparticles and DNA. Since the DNA−chitosan interaction was preserved at pH above the pK_a, we attempted to capture DNA at pH 8.5.

Capture of pUC19 and *E. coli* genomic DNA in a pH 8.5 Tris buffer using chitosan microparticles was just as efficient as capture at the lower pH (Figure 3). Using just 40 μg of particles, up to 3 μg (10^{12} copies) of pUC19 and 0.6 ng (10^5 copies) of genomic *E. coli* DNA were separately loaded onto the particles (increased amounts of *E. coli* genomic DNA were

not attempted). Given that 100% of the pUC19 DNA was captured for 3 μg of loaded DNA (and all loaded values below this mass as well), we believe that the full loading capacity of the particles was not reached. Yet this partial loading capacity of the chitosan microparticles is an order of magnitude greater than previously reported for chitosan-coated and bare silica beads.[7] As with low pH capture, pUC19 DNA and *E. coli* genomic DNA could not be eluted off the particles using extreme elution protocols.

DNA captured onto chitosan at pH above the pK_a has not been reported before. This is significant because nucleic acid assays are typically performed at a pH of around 8.5. Thus, DNA extraction could be performed on a sample using the same buffer that is used for PCR, next generation sequencing, isothermal amplification techniques, aptamer-based assays, or enzymatic assays. Extracting DNA with a single buffer would reduce reagents, decrease sample preparation time, and simplify micro total analysis systems.

Chemical Mechanism for Capture above pK_a. Adsorption of DNA to chitosan at a pH above the pK_a is counterintuitive. Previous work has shown capture of DNA to be effective only at pH lower than 7.5; at pH 8, a sharp increase in DNA elution was observed.[7] We aimed to elucidate the mechanism behind the phenomenon of capture at pH 8.5 by measuring the adsorption of an anionic dye, brilliant yellow (BY), as a function of pH (Figure 4).
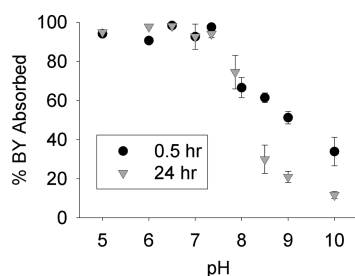

Figure 4. Adsorption of brilliant yellow dye onto chitosan particles cross-linked for 30 min and 24 h. Error bars represent the standard deviation for *n* = 3.

It was found that chitosan microparticles were still pH-responsive, but that the amines are still ionized at pH well above the pK_a of free chitosan in solution (6.4). The microparticles captured nearly 100% of the added dye at pH 7.5 and below, while above pH 7.5, the BY adsorption began to decrease. The magnitude of the pH response was enhanced for microparticles that were cross-linked for 24 h, which showed significantly lower BY adsorption as compared to microparticles cross-linked for 30 min (at pH above 8). Also, the adsorbed dye was not released from either microparticle system when washed in higher pH buffers. In control experiments, methylene blue, a cationic dye, did not adsorb at all, verifying that BY interactions were likely electrostatic. Taken together, these results show that the chitosan microparticles still carry a positive charge at pH 8.5 (in the presence of the BY) and that increased cross-linking reacted away protonatable amine groups.

BY is a small molecule and thus has the potential to diffuse into the microparticles to adsorb. To distinguish the electrostatic potential at the outer surface from the inner core of the microparticles, we investigated the adsorption of negatively charged gold nanoparticles, approximately 30 nm in diameter. At pH 6, 20% of nanoparticles added were adsorbed, while only

5% of the nanoparticles adsorbed at pH 8.5. As gold nanoparticles are not able to penetrate into a cross-linked chitosan matrix, they would be restricted to the outer surface of the microparticles. Because glutaraldehyde cross-linking occurs from the outer surface inward, there are fewer protonated amines available at the surface of the microparticles as compared to below the surface. Interestingly, it appears that the unreacted amines (which are limited due to glutaraldehyde cross-linking) on the outer surface of the microparticles are charged at pH 6, but mostly uncharged at pH 8.5, exhibiting a behavior similar to chitosan in solution (i.e., a pK_a of 6.4).

Because the microparticles are produced by glutaraldehyde cross-linking from the outside in, as microparticles are cross-linked over longer times, the thickness of the shell of reacted amines around the microparticle increases. A relatively large shell thickness of reacted amines would diminish the interaction and make it difficult for macromolecules to access the ionizable amines. The decrease in capture efficiency of pUC19 at pH 8.5 for increasingly cross-linked chitosan microparticles is shown in Figure 5. The capture efficiency remained high with up to 16 h
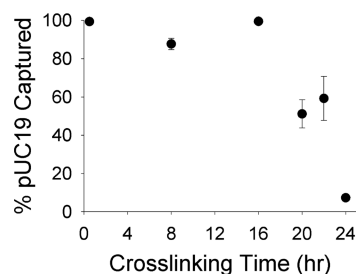

Figure 5. Capture efficiency of pUC19 as a function of cross-linking time. Over time, an appreciable shell of amines were cross-linked around the chitosan particle and pUC19 was not adsorbed.

of cross-linking. Long cross-linking times with glutaraldehyde were required, probably due to limited transport of cross-linker from mineral oil, through surfactant-surrounded droplets, and into the chitosan droplets/particles (log K_{ow} = −0.18).[24] Cross-linking longer, up to 22 h, resulted in about 50% pUC19 capture, while with 24 h of cross-linking, pUC19 capture was reduced to an insignificant 7%. This suggests that, as the shell of reacted amines increases, pUC19 DNA is not captured as efficiently.

To summarize these results together, (i) the amine groups of the nanoporous chitosan microparticles appear to be ionized even at pH values above the chitosan pK_a when interacting with a small anionic molecule, (ii) the microparticles exhibit a pH-dependent ionization that is more typical of chitosan in solution when interacting with anionic nanoparticles that cannot interact with the chitosan below the surface, and (iii) as the shell of cross-linked chitosan increases in thickness, capture of pUC19 becomes less efficient. Thus, we hypothesize that just below the surface of the microparticle the amine groups are largely still charged at pH 8.5 (in the presence of DNA), enabling capture of DNA substructures that penetrate below the surface. In fact, it has been shown previously that in a dense chitosan microenvironment the pK_a can be shifted in the presence of anionic molecules, including nucleic acids,[16,17] thus, explaining the results of Figures 3 and 4.

While BY may penetrate well into the core of the microparticle, plasmid DNA would not be expected to penetrate deeply. The pore size radius of chitosan membranes

cross-linked with glutaraldehyde has been approximated to be 1 nm by measuring solute diffusion.[22] The radius of gyration of supercoiled pUC19 is about 170 nm, so it would not be possible for the plasmid to be absorbed into the core of the bead. Instead, a small fragment of a DNA chain could condense, interact with unreacted amines below the outer surface (where the density of amine groups is greater), and become entangled with chitosan chains. Indeed, it has been reported that pUC19 in complexes with chitosan does compact to less than one-half the size of free pUC19.[23] Thus, we believe that substructures of DNA are captured below the surface of the microparticle through electrostatic interactions and are permanently retained through a combination of electrostatic and steric interactions.

qPCR Directly from Chitosan Microparticles. The aim of this work is to simplify the PCR preparation process to the minimal number of steps, which can be accomplished if DNA can be amplified directly from the microparticle (i.e., without elution). Results of direct qPCR (i.e., captured template amplified directly off of the microparticle) are presented in Figure 6 and compared with typical solution-based qPCR. PCR
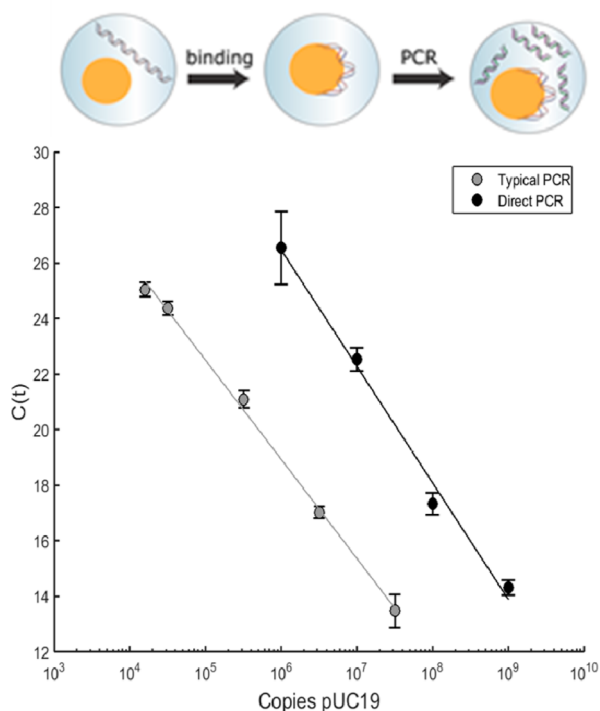

Figure 6. PCR calibration curves of direct PCR (DNA amplified directly from the microparticle, as indicated above the graph) and typical solution-based PCR.

products were verified to be correct by gel electrophoresis (Supporting Information, Figure S1) and melt analysis (Supporting Information, Figure S2). It is clear that the DNA that has been captured electrostatically onto the chitosan microparticles is still accessible by primers and polymerase for amplification and that the PCR reaction is relatively efficient. The calibration curve, shown in Figure 6, was constructed from standard samples of pUC19 and found to be linear over 4 orders of magnitude. The efficiency of direct qPCR was 67.6% (the efficiency of amplifications with pUC19 directly added to the reaction in solution was 90.6%). As a result, for direct PCR,

about 4−8 extra cycles were required, which only translates to an extra 5−10 min of reaction time.

To gain more insight into the performance difference between PCR directly from the microparticles and solution-based PCR, the real-time amplification curves are presented in Figure 7. The delay in cycle threshold is apparent, and in
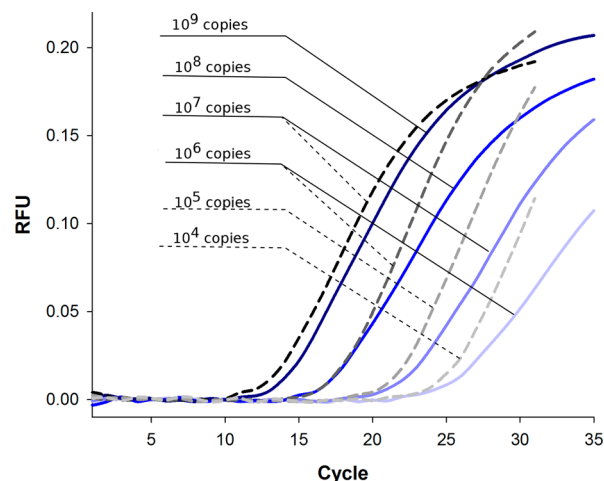

Figure 7. Fluorescence intensity at each cycle from sets of calibration curves in Figure 6. The amplification of reactions with 0.5 h cross-linked particles with 10^9, 10^8, 10^7, and 10^6 initial adsorbed copies of pUC19 from left to right are shown in blue solid lines. The amplification of 10^7, 10^6, 10^5, and 10^4 copies pUC19 initially added to the reaction from left to right are shown in black dashed lines. The direct PCR amplification is slower than solution-based reactions.

addition, the rate of increase in fluorescence was greater in solution-based PCR than direct PCR for comparable DNA copy numbers. Possible explanations for the differential performance include adsorption of polymerase, primers, or amplicons to the microparticles, as well as inaccessibility of the template due to either the binding of the DNA template or the packing of the microparticles during PCR.

To determine whether direct PCR is affected by the loss of Taq polymerase binding at the chitosan surface, 3× Taq was utilized in a reaction and compared with 1× Taq. As shown in Supporting Information, Figure S3, the cycle thresholds for the 1× and 3× cases are nearly equivalent (the saturation intensity is higher, but this is also typical of solution-based PCR with high Taq concentration).

To determine whether primers are lost due to binding onto the chitosan, PCR reactions were performed with the supernatant of a primer solution that was mixed with chitosan microparticles. When mixing the primers and microparticles by aspirating with a pipet, which is a typical method to prepare a PCR reaction, the recovered primers efficiently amplified pUC19 plasmid DNA (in solution), indicating that little if any primers were lost to adsorption onto the microparticles (Supporting Information, Figure S4). Note that when solutions of primers were vortexed with the microparticles for 3 min, the subsequent reaction did not amplify DNA, suggesting that primers were permanently captured by the chitosan micro-particles (recall that plasmid and genomic DNA are captured under vortexing conditions).

One likely explanation for the delay in cycle threshold (Figure 6) and the decrease in amplification speed (Figure 7) is that amplicons that are produced during PCR do not escape the

packed beads during amplification, reducing the reaction efficiency and the measured fluorescence signal. The trend in Figure 7 supports this, as higher loading concentrations of plasmid DNA lead to a faster rate of accumulation of the signal, suggesting that lower available surface area leads to more efficient amplification. In future work, one could investigate various surface blocking strategies (following DNA capture) to keep amplicons in solution.

Finally, the inaccessibility of plasmid or genomic DNA upon packing the beads during the PCR reaction is also plausible but is difficult to assess. The microparticles, which are on the order of a few microns in diameter, can be packed relatively tightly during the PCR reaction when the magnet pulls them to the side of the well. Even without the magnet, it is easily visible that the beads settle to the bottom, also packing. In either case, we may assume that a significant fraction of the captured DNA is inaccessible due to microparticles packing against each other, leading to a lower apparent number of DNA templates for amplification and, thus, a higher cycle threshold as compared to conventional solution-based PCR. In future work, we propose to address this by combining this sample preparation technique with digital PCR when attempting to amplify low copy numbers of DNA. By separating individual microparticles into aqueous droplets, the entire surface of the microparticle is accessible by polymerase; we anticipate that this will lead to a substantial improvement in amplification performance for the direct PCR technique.

CONCLUSION

To our knowledge, this work demonstrates the first reported methodology for DNA capture and direct amplification in a single PCR-compatible buffer. Chitosan magnetic particles were produced by an emulsion cross-linking process. These particles were capable of DNA extraction but behaved drastically different from previously published extraction schemes relying on chitosan-surface charge-switching. The microarticles adsorbed DNA at a pH optimal for PCR (above the pK_a of chitosan) and did not elute the DNA after (i) high salt, (ii) high pH, or (iii) high temperature treatments. After glutaraldehyde cross-linking for 30 min, the microparticles were still found to be pH-responsive, but the majority of the amine groups were still apparently ionized at a pH values higher than the reported chitosan pK_a of 6.4. Further cross-linking longer than 16 h resulted in decreased DNA adsorption. We believe that DNA was electrostatically and sterically bound to the interior of the microparticle. DNA was not eluted off of the particles during washes, enabling the direct amplification of DNA sequences from the microparticles in the PCR reaction, In future work, methodologies for improving the efficiency of the direct PCR reaction will be investigated. In addition, cell lysis capabilities will be assessed, with an aim of a completely hands-free sample-to-answer PCR methodology for near-patient diagnostics.

ASSOCIATED CONTENT

Ⓢ Supporting Information

The Supporting Information is available free of charge on the ACS Publications website at DOI: 10.1021/acs.analchem.5b03006.

Product melt peaks and gels, as well as PCR results investigating reasons for the shift in cycle threshold for direct PCR (PDF).

AUTHOR INFORMATION

Corresponding Author

*E-mail: ianwhite@umd.edu.

Author Contributions

†These authors contributed equally (K.R.P. and I.A.N.).

Notes

The authors declare no competing financial interest.

REFERENCES

(1) Boom, R.; Sol, C. J.; Salimans, M. M.; Jansen, C. L.; Wertheim-van Dillen, P. M.; van der Noordaa, J. *J. Clin. Microbiol.* **1990**, *28* (3), 495−503.

(2) Miller, D. N.; Bryant, J. E.; Madsen, E. L.; Ghiorse, W. C. *Appl. Environ. Microbiol.* **1999**, *65* (11), 4715−4724.

(3) Haugland, R. A.; Brinkman, N.; Vesper, S. J. *J. Microbiol. Methods* **2002**, *50* (3), 319−323.

(4) Naccache, S. N.; Hackett, J.; Delwart, E. L.; Chiu, C. Y. *Proc. Natl. Acad. Sci. U. S. A.* **2014**, *111* (11), E976−E976.

(5) Roy, E.; Stewart, G.; Mounier, M.; Malic, L.; Peytavi, R.; Clime, L.; Madou, M.; Bossinot, M.; Bergeron, M. G.; Veres, T. *Lab Chip* **2015**, *15* (2), 406−416.

(6) Kneuer, C.; Sameti, M.; Haltner, E. G.; Schiestel, T.; Schirra, H.; Schmidt, H.; Lehr, C.-M. *Int. J. Pharm.* **2000**, *196* (2), 257−261.

(7) Cao, W.; Easley, C. J.; Ferrance, J. P.; Landers, J. P. *Anal. Chem.* **2006**, *78* (20), 7222−7228.

(8) Hagan, K. A.; Meier, W. L.; Ferrance, J. P.; Landers, J. P. *Anal. Chem.* **2009**, *81* (13), 5249−5256.

(9) Liu, C.-J.; Lien, K.-Y.; Weng, C.-Y.; Shin, J.-W.; Chang, T.-Y.; Lee, G.-B. *Biomed. Microdevices* **2009**, *11* (2), 339−350.

(10) Agirre, M.; Zarate, J.; Ojeda, E.; Puras, G.; Desbrieres, J.; Pedraz, J. L. *Polymers* **2014**, *6* (6), 1727−1755.

(11) Alameh, M.; DeJesus, D.; Jean, M.; Darras, V.; Thibault, M.; Lavertu, M.; Buschmann, M. D.; Merzouki, A. *Int. J. Nanomed.* **2012**, *7*, 1399−1414.

(12) Jiang, C.; Xu, S.; Zhang, S.; Jia, L. *Anal. Biochem.* **2012**, *420* (1), 20−25.

(13) Kim, J.; Mauk, M.; Chen, D.; Qiu, X.; Kim, J.; Gale, B.; Bau, H. H. *Analyst* **2010**, *135* (9), 2408−2414.

(14) Oblath, E. A.; Henley, W. H.; Alarie, J. P.; Ramsey, J. M. *Lab Chip* **2013**, *13* (7), 1325−1332.

(15) Sun, Y.; Quyen, T. L.; Hung, T. Q.; Chin, W. H.; Wolff, A.; Bang, D. D. *Lab Chip* **2015**, *15* (8), 1898−1904.

(16) Ma, P. L.; Buschmann, M. D.; Winnik, F. M. *Anal. Chem.* **2010**, *82* (23), 9636−9643.

(17) Ma, P. L.; Lavertu, M.; Winnik, F. M.; Buschmann, M. D. *Biomacromolecules* **2009**, *10* (6), 1490−1499.

(18) Hermanson, G. *Bioconjugate Techniques*, 2nd ed.; Elsevier, Inc.: London, 2008.

(19) Hoppmann, E. P.; Yu, W. W.; White, I. M. *Methods* **2013**, *63* (3), 219−224.

(20) Reedy, C. R.; Price, C. W.; Sniegowski, J.; Ferrance, J. P.; Begley, M.; Landers, J. P. *Lab Chip* **2011**, *11* (9), 1603.

(21) Kendall, E. L.; Wienhold, E.; DeVoe, D. L. *Biomicrofluidics* **2014**, *8* (4), 044109.

(22) Krajewska, B.; Olech, A. *Polym. Gels Networks* **1996**, *4* (1), 33−43.

(23) Lai, E.; van Zanten, J. H. *Biophys. J.* **2001**, *80* (2), 864−873.

(24) Emmanuel, E.; Hanna, K.; Bazin, C.; Keck, G.; Clément, B.; Perrodin, Y. *Environ. Int.* **2005**, *31* (3), 399−406.

Capture and direct amplification of DNA on chitosan microparticles in a single PCR-optimal solution.

Kunal R. Pandit*, Imaly A. Nanayakkara†, Weidong Cao,†† Srinivasa R. Raghavan*,†, Ian M. White†.

*Department of Chemical & Biomolecular Engineering. University of Maryland, College Park, MD

†Fischell Department of Bioengineering, University of Maryland, College Park, MD

††Canon US Life Sciences, Inc., Rockville MD.

Supporting Information

The supporting information includes product melt peaks and gels for amplicon validation, as well as PCR results investigating reasons for the shift in cycle threshold for direct PCR.
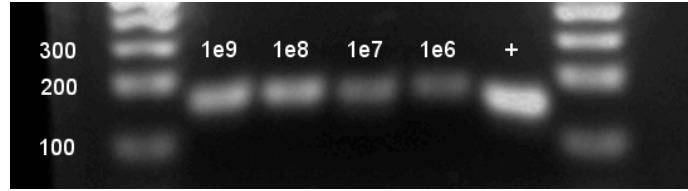
Figure S1. Direct PCR products run on a 1% agarose gel and stained with SYBR Green I. Copies of pUC19 captured by beads in reactions from Fig. 6 are listed above each lane; the positive control lane (+) contains product from solution-based PCR, and DNA ladders are in the first and last lanes.
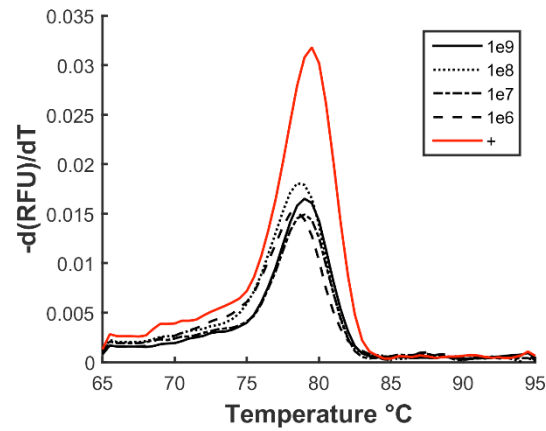

Figure S2. Melt curves from one calibration curve of PCR products from Fig. 6. The melt temperatures, 79.0 ± 0.5 °C, of the amplicons with beads in solution ($10^9 - 10^6$) match the melt temperature, 79.5 °C, of amplicons generated without beads (+).
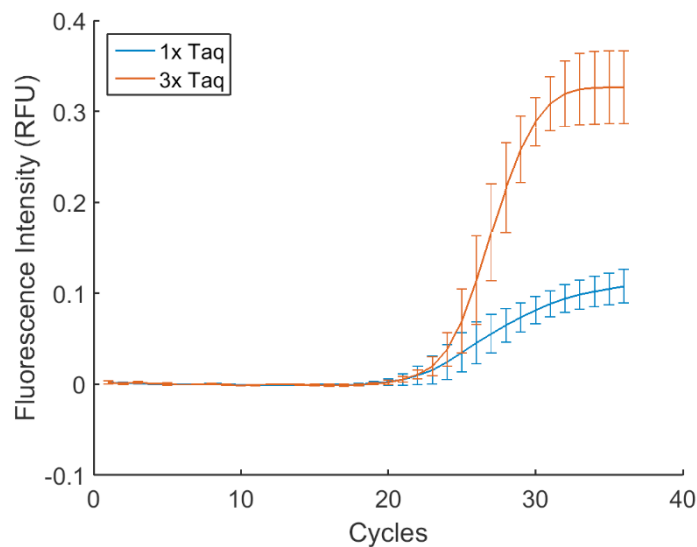
Figure S3. Amplification curves of 10^6 copies of pUC19 on chitosan beads with 1X or 3X Taq polymerase. Cycle thresholds determined for 1X and 3X polymerase were 24.06 ± 1.95 and 23.24 ± 0.82, respectively. Error bars represent the standard deviation for n = 3.
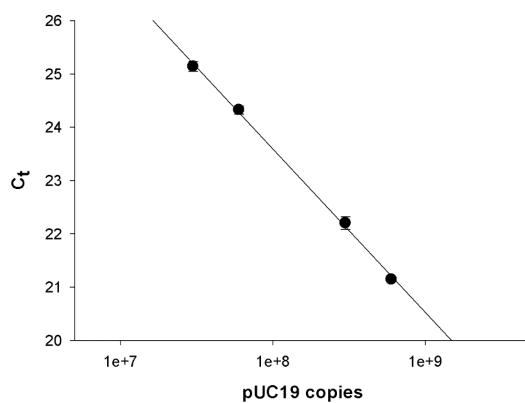

Figure S4. PCR calibration curve constructed from primers that had been first aspirated with chitosan microparticles before being added to the solution-based PCR reaction. The efficiency of the reaction was 112%, suggesting that minimal primers were absorbed onto the chitosan microparticles.